Journal of Molecular Catalysis A: Chemical 326 (2010) 113–120

Contents lists available at ScienceDirect

Journal of Molecular Catalysis A: Chemical

journal homepage: www.elsevier.com/locate/molcata

Preparation and characterization of the chirally modified rapidly quenched skeletal Ni catalyst for enantioselective hydrogenation of butanone to R-(−)-2-butanol

Zhiying Lou[a], Xueying Chen[a], Li Tian[a], Minghua Qiao[a,*], Kangnian Fan[a], Heyong He[a,*], Xiaoxin Zhang[b], Baoning Zong[b]

[a] Department of Chemistry, Shanghai Key Laboratory of Molecular Catalysis and Innovative Materials, Fudan University, No. 220 Handan Road, Shanghai 200433, PR China
[b] State Key Laboratory of Catalytic Material and Chemical Engineering, Research Institute of Petroleum Processing, SINOPEC, Beijing 100083, PR China

ARTICLE INFO

Article history:
Received 12 February 2010
Received in revised form 26 April 2010
Accepted 28 April 2010
Available online 6 May 2010

Keywords:
Rapid quenching
Skeletal Ni
Tartaric acid
Butanone
Enantioselective hydrogenation

ABSTRACT

A rapidly quenched skeletal Ni (RQ Ni) prepared by the melt-spinning method followed by alkali leaching was used as a new category of Ni precursor to fabricate effective chiral Ni catalyst. A series of tartaric acid (TA)–NaBr–modified RQ Ni catalysts (MRQNi) were derived, and the textural and structural properties of the MRQNi catalysts were systematically investigated. It is found that the modification conditions influence profoundly the composition, texture, and Ni crystallite size of the MRQNi catalysts. In liquid phase hydrogenation of butanone to R-(−)-2-butanol, the optimized MRQNi catalyst exhibits much better activity and enantioselectivity than the similarly chirally modified Raney Ni catalyst. Based on the characterizations, the superior catalytic performance of the MRQNi catalyst is mainly attributed to the higher surface content of the sodium–nickel(II) tartrate complex than that on the chirally modified Raney Ni catalyst.

© 2010 Elsevier B.V. All rights reserved.

1. Introduction

There is a growing interest in the synthesis of optically pure chiral substances especially in the pharmaceutical, agrochemical, and perfume industries [1,2]. Currently, the sales of single isomer drugs have already accounted for about half of the total drug sales worldwide [3]. Among many strategies established to this end, enantioselective hydrogenation over a heterogeneous catalyst is one of the promising routes owing to its inherent operational and economical advantages [4]. Up to now, one of the most intensively studied chiral catalytic systems is the TA–NaBr–modified Ni catalyst (MNi) [5–10], which has been demonstrated effective for the enantioselective hydrogenation of pre-chiral β-ketoesters, β-diketones, and 2-alkanones to chiral alcohols [5–18]. It was found that nickel materials suitable as precursors for the preparation of the MNi catalysts mainly fall in the following three categories: Raney Ni leached from commercial Ni–Al alloy [11–13], Ni black reduced from pure nickel oxide or nickel carbonate [14–16], and commercial Ni powder [17] or fine Ni powder condensed from Ni vapor in vacuum [10]. For enantioselective hydrogenation of 2-alkanones, such as 2-octanone, chirally modified Raney Ni (M-Raney Ni) is more effective for achieving higher hydrogenation activity and enantioselectivity than pure Ni powder [7,10,18].

Recently, the introduction of the rapid quenching technique to the preparation of the Ni–Al alloy has exerted a substantial impact on catalytic investigations [19–26]. Explorations demonstrated that after alkali leaching, the resulting RQ Ni catalyst exhibited higher activity and selectivity for the hydrogenation of olefinic, carbonyl, and nitryl groups than the commercial Raney Ni catalyst [22,24,25]. As compared to Raney Ni that is leached from the naturally solidified Ni–Al alloy, more defects are present in the rapidly quenched Ni–Al alloy (RQ Ni–Al), leading to coordinatively more unsaturated Ni crystallites in RQ Ni. Such crystallites are more beneficial for the adsorption and activation of the reactants [21]. Moreover, RQ Ni has larger Ni crystallite size than Raney Ni [24]. It has been proposed that larger Ni crystallites tend to afford MNi catalysts better enantioselective hydrogenation ability [16,27]. Thus, it will be very attractive to use RQ Ni as a new category of Ni precursor to formulate a novel MNi catalyst for enantioselective hydrogenation.

In this paper, we prepared a series of TA–NaBr–modified RQ Ni catalysts (MRQNi) by pre-modification of RQ Ni in an aqueous solution containing (2S,3S)-(−)-TA and NaBr, and examined their catalytic performances in the enantioselective hydrogenation of butanone. The M-Raney Ni catalyst was prepared according to the

* Corresponding authors. Tel.: +86 21 65643916; fax: +86 21 6562978.
E-mail addresses: mhqiao@fudan.edu.cn (M. Qiao), heyonghe@fudan.edu.cn (H. He).

1381-1169/$ – see front matter © 2010 Elsevier B.V. All rights reserved.
doi:10.1016/j.molcata.2010.04.018

typical modification condition of Raney Ni reported in the literature for comparison [5,28]. Based on systematic characterizations, it is found that the modification conditions influenced significantly the composition, texture, and crystallite size of the MRQNi catalysts. The activity and enantioselectivity of the MRQNi catalysts in the liquid phase hydrogenation of butanone with respect to the modification conditions and reaction variables are reported.

2. Experimental

2.1. Catalyst preparation

The RQ Ni–Al alloy was prepared by a single roller melt-spinning technique. The details are described in our previous work [24]. The MRQNi catalysts were prepared by the following procedure. Exactly 1 g of the RQ Ni–Al alloy was treated with 10 ml of 6.0 M NaOH solution at 363 K for 1 h under stirring to leach out Al. The resulting black solid was washed with distilled water until neutrality. Then, the as-prepared RQ Ni was soaked in an aqueous solution with different volume but the same amount of (2S,3S)-(−)-TA of 0.4 g and a desired amount of NaBr, and stirred gently for 1 h at a predetermined temperature in a three-necked flask fitted with a condenser. Prior to modification, the pH of the modification solution was adjusted to 3.2 using a NaOH aqueous solution. The MRQNi catalysts were labeled MRQNi-*x*-*y*-*z*, where *x* refers to the weight of NaBr in the modification solution; *y*, the volume of the modification solution; and *z*, the modification temperature in K. For example, MRQNi-9-10-413 denotes the RQ Ni catalyst modified in 10 ml aqueous solution containing 9.0 g NaBr at 413 K. After modification, the supernatant was decanted, and the resulting MRQNi catalyst was washed with distilled water three times, followed with methanol three times to replace water. The catalyst was stored in methanol for characterization and activity test.

The M-Raney Ni catalyst was leached from a commercially available Ni–Al alloy (Ni/Al, 50/50, w/w, Shanghai Chemical Corp.) and modified according to the reported optimal condition [5,28]. In brief, after alkali leaching, Raney Ni was soaked in 40 ml aqueous solution containing 0.4 g (2S,3S)-(−)-TA and 6.0 g NaBr at 373 K for 1 h. It should be cautioned that since RQ Ni and Raney Ni are pyrophoric, care must be taken to preclude air oxidation during sample handling and disposal.

2.2. Characterization

The Ni and Al compositions of the catalyst were determined by inductively coupled plasma-atomic emission spectroscopy (ICP-AES; Thermo Elemental IRIS Intrepid). The multipoint Brunauer–Emmett–Teller surface area (S_{BET}) and pore size distribution (PSD) were acquired on a Micromeritics TriStar3000 apparatus using N_2 physisorption at 77 K. Prior to the measurement, the catalyst was transferred to a glass adsorption tube and degassed at 383 K under N_2 flow for 2 h. The pore volume was calculated from the amount of N_2 adsorbed at a relative pressure of 0.995. The PSD curve was calculated from the desorption branch of the isotherms using the Barrett–Joyner–Halenda (BJH) algorithm [29]. The surface morphology was observed by scanning electron microscopy (SEM; Philips XL30). Before being transferred into the SEM chamber, the catalyst with methanol was dispersed on the sample holder and quickly moved into the vacuum evaporator, in which a thin gold layer was deposited after being dried in vacuo. The powder X-ray diffraction (XRD) pattern was collected on a Bruker AXS D8 Advance X-ray diffractometer using Cu Kα radiation (λ = 0.15418 nm). The tube voltage was 40 kV, and the current was 40 mA. The catalyst with methanol was loaded in the in situ cell, with Ar flow (99.9995%) purging the cell during the detection to avoid oxidation. The mean Ni crystallite size was obtained from the integral width of the Ni(1 1 1) reflection using the Scherrer relation after correction for instrumental broadening with the Warren procedure [30,31].

In order to reveal the nature of the tartrate species formed on the MRQNi catalyst, the thermal decomposition behavior of the surface species on the MRQNi catalyst was compared with those of the nickel(II) tartrate and sodium–nickel(II) tartrate complexes synthesized according to Kukula and Červený [32] by thermogravimetric analysis (TGA; Perkin Elmer TGA7). The heating rate was 10 K min^{-1}, and the N_2 flow rate was 10 ml min^{-1}.

The surface composition and chemical state were detected by X-ray photoelectron spectroscopy (XPS; Perkin Elmer PHI5000C) using Mg Kα line ($h\nu$ = 1253.6 eV) as the excitation source. The sample was pressed into a self-supported disc, mounted on the sample stage, degassed in the pretreatment chamber at 383 K for 2 h in vacuo, and then transferred into the analyzing chamber where the background pressure was better than 2×10^{-9} Torr. All the binding energy (BE) values were referenced to the C 1s peak of contaminant carbon at 284.6 eV. For quantitative purpose, the intensity of the photoelectron peak was integrated after being subtracted a Shirley-shaped background.

2.3. Catalytic testing and product analysis

The hydrogenation reaction was carried out in a 100 ml mechanically stirred stainless steel autoclave at desired reaction temperature and H_2 pressure. Other reaction conditions were as follows: 1.0 ml of butanone, 20 ml of methanol, 0.5 g of the catalyst, 1.8 g of pivalic acid, and a stirring rate of 800 rpm to exclude diffusion limitations. It is known that pivalic acid can effectively facilitate tartaric acid to recognize the structures of 2-alkanone by expelling the bulky alkyl group of the substrate [7]. Conversion and enantiomeric excess (ee) were determined on a gas chromatograph equipped with a CP-Chirasil-Dex CB capillary column (25 m × 0.25 mm × 0.25 μm) and a flame ionization detector (FID) at 318 K. N_2 was used as the carrier gas. The ee value was expressed as:

$$\text{ee}\,(\%) = \frac{[\text{R-(}-\text{)-2-butanol}] - [\text{S-(}+\text{)-2-butanol}]}{[\text{R-(}-\text{)-2-butanol}] + [\text{S-(}+\text{)-2-butanol}]} \times 100.$$

The assignments of the absolute configurations of the products were based on the retention time of authentic R-(−)-2-butanol (Aldrich) and racemic 2-butanol (Shanghai Chemical Corp.) reagents. It should be noted that in this work that we did not express the activity in turnover frequencies per site or so on, because it is infeasible to determine the number of active sites on these chirally modified catalysts.

3. Results and discussion

3.1. Catalyst composition

The bulk Ni and Al contents in the RQ Ni and Raney Ni catalysts before and after chiral modification are given in Table 1. Since it has been proposed that the enantioselectivity of the MNi catalyst is related to the surface Ni/Al ratio [14], we also calculated the surface Ni and Al contents by means of XPS. According to Table 1, the bulk and surface Ni and Al contents of RQ Ni are similar, with the amount of Al being ca. 21 wt% both in the bulk and on the surface. Raney Ni has a lower bulk Al content than RQ Ni, while its surface Al content is higher. After modification, irrespective of the modification conditions, all the MRQNi catalysts retained ca. 2/3 of the initial amount of Al in the bulk. However, the surface Al contents of the MRQNi catalysts deviated remarkably from the bulk ones, with much less Al on the surface. The reason that Al was preferentially removed from the surface is possibly due to the fact that the resid-

Table 1
Physicochemical properties of the chirally modified skeletal Ni catalysts.

Catalyst	Bulk comp. (wt%)	Surf. comp. (wt%)	S_{BET} ($m^2\ g^{-1}$)	V_{pore} ($cm^3\ g^{-1}$)	d_{pore} (nm)	$d_{cryst.}$ (nm)
RQ Ni	$Ni_{78.8}Al_{21.2}$	$Ni_{79.3}Al_{21.7}$	90	0.10	4.6	6.8
Raney Ni	$Ni_{81.7}Al_{18.3}$	$Ni_{75.3}Al_{24.7}$	78	0.10	3.9	5.6
M-Raney Ni	$Ni_{89.1}Al_{10.9}$	$Ni_{99.6}Al_{0.4}$	29	0.21	21.7	14.2
MRQNi-9-40-373	$Ni_{85.8}Al_{14.2}$	$Ni_{92.5}Al_{7.5}$	47	0.15	12.4	8.7
MRQNi-9-40-383	$Ni_{85.7}Al_{14.3}$	$Ni_{94.5}Al_{5.5}$	40	0.13	14.3	9.0
MRQNi-9-40-393	$Ni_{85.6}Al_{14.4}$	$Ni_{96.4}Al_{3.6}$	35	0.12	16.5	10.2
MRQNi-9-40-403	$Ni_{85.5}Al_{14.5}$	$Ni_{97.6}Al_{2.4}$	30	0.10	18.1	12.5
MRQNi-9-40-413	$Ni_{85.4}Al_{14.6}$	$Ni_{98.0}Al_{2.0}$	26	0.09	19.4	14.2
MRQNi-9-30-413	$Ni_{85.6}Al_{14.4}$	$Ni_{98.6}Al_{1.4}$	21	0.09	14.2	14.3
MRQNi-9-20-413	$Ni_{85.8}Al_{14.2}$	$Ni_{99.4}Al_{0.6}$	18	0.08	12.0	14.5
MRQNi-9-10-413	$Ni_{86.0}Al_{14.0}$	$Ni_{99.8}Al_{0.2}$	18	0.08	10.9	14.6

ual non-stoichiometric Ni_2Al_3 phase in the bulk of RQ Ni is very resistant to corrosion [20,24,33,34]. For Raney Ni, after modification more Al was leached away from the bulk, attributable to the more facile removal of hydrated alumina adsorbed in the pores of Raney Ni [11].

In Table 1, it is also found that the higher the modification temperature, the lower is the surface Al content in the MRQNi catalysts. When the modification temperature was elevated to 413 K, the surface Al content was decreased to 0.2 wt% (entry 11, Table 1). On the other hand, higher concentration of the modification solution resulted in lower surface Al content. For example, the surface Al content decreased monotonically from 2 wt% for MRQNi-9-40-413 to 0.2 wt% for MRQNi-9-10-413.

3.2. Catalyst texture

Fig. 1a illustrates the N_2 physisorption isotherms of Raney Ni, M-Raney Ni, RQ Ni, and MRQNi-9-10-413 as a representative of the MRQNi catalysts, since the isotherms of the MRQNi catalysts are similar. Raney Ni and RQ Ni exhibited a type E isotherm according to de Boer's classification [35], indicating the ink-bottle pore shape of both the unmodified catalysts. After modification, the isotherms changed to type A, indicating that the pore shape of the chirally modified Ni catalysts changed to the open-ended cylindrical pore shape [35]. The corresponding PSD curves of the above catalysts are plotted in Fig. 1b. Raney Ni exhibited only one maximum at 3.6 nm, while RQ Ni exhibited a bimodal distribution with a small maximum at 2.4 nm and a large one at 3.6 nm. After modification, the features of both Raney Ni and RQ Ni almost diminished, and a new maximum at much larger pore diameter emerged. Detailed analysis of the PSD curves of the MRQNi catalysts revealed that the new maximum depended on the modification condition and varied in the range of 8–15 nm. As compared to MRQNi, the maximum on the PSD curve of M-Raney Ni shifted to a much larger diameter of ~23 nm, presumably due to the more facile removal of the hydrated alumina from Raney Ni.

The textural properties of Raney Ni and RQ Ni before and after chiral modification are summarized in Table 1. RQ Ni exhibited a BET surface area of 90 $m^2\ g^{-1}$ and an average pore diameter of 4.6 nm, which are larger than those of Raney Ni (78 $m^2\ g^{-1}$, 3.9 nm), while their pore volumes are similar. After modification, the BET surface areas of the MRQNi and M-Raney Ni catalysts were decreased as compared to those of RQ Ni and Raney Ni. The modification temperature has a distinct effect on the BET surface areas of the MRQNi catalysts. As shown in Table 1, the BET surface areas of the MRQNi-9-40-*z*-series catalysts decreased from 47 to 26 $m^2\ g^{-1}$ when the modification temperature was raised from 373 to 413 K. The BET surface areas of the MRQNi catalysts also varied with the concentration of the modification solution. Table 1 shows that the BET surface areas decreased steadily from 26 $m^2\ g^{-1}$ for MRQNi-9-40-413 to 18 $m^2\ g^{-1}$ for MRQNi-9-10-413 when the modification solution became more concentrated.

The modification temperature and the concentration of the modification solution influenced the pore volumes of the MRQNi catalysts as well. Higher modification temperature (entries 4–8, Table 1) and concentration of the modification solution (entries 8–11, Table 1) led to smaller pore volume. And when the modification temperatures were below 403 K, the pore volumes of the MRQNi catalysts were larger than that of RQ Ni, but further elevating the modification temperature led to pore volumes smaller than that of RQ Ni. For Raney Ni, after modification, the pore volume increased from 0.10 to 0.21 $cm^3\ g^{-1}$, attributable again to the more facile removal of the hydrated alumina blocking the pores of Raney Ni [11].

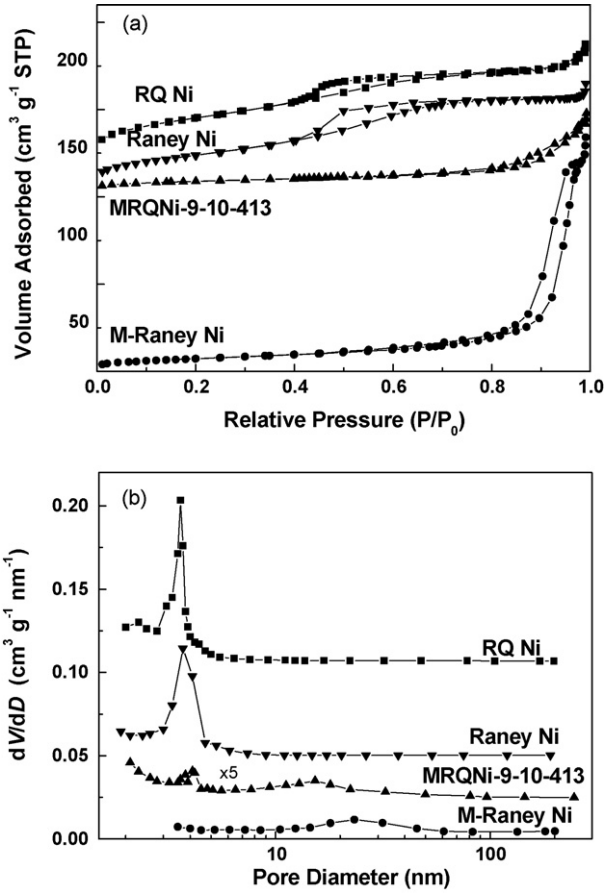

Fig. 1. (a) N_2 adsorption–desorption isotherms and (b) pore size distribution curves of the RQ Ni, Raney Ni, M-Raney Ni, and MRQNi-9-10-413 catalysts.

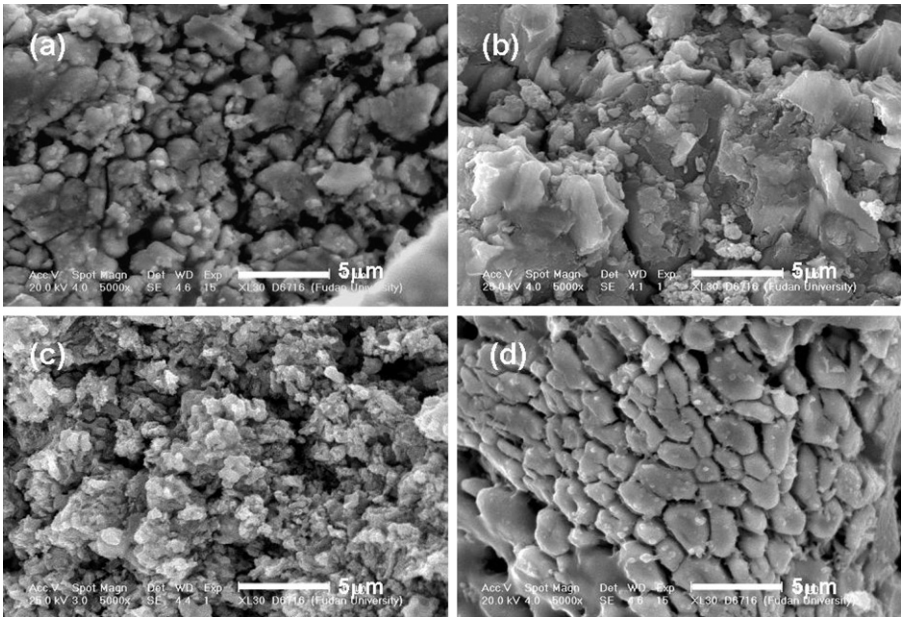

Fig. 2. SEM images of the (a) RQ Ni, (b) Raney Ni, (c) MRQNi-9-10-413, and (d) M-Raney Ni catalysts.

3.3. Morphology and structure

Figure 2 shows the SEM images of RQ Ni and MRQNi-9-10-413 as a representative of the MRQNi catalysts. For comparison, the SEM images of Raney Ni and M-Raney Ni are presented. It is found that the particles of RQ Ni and MRQNi-9-10-413 displayed round contour rather than the angular morphology of Raney Ni and M-Raney Ni. After modification, the particles of MRQNi-9-10-413 and M-Raney Ni became smaller and less compact than those of RQ Ni and Raney Ni, which is consistent with the morphology change between TA–NaBr–modified Raney Ni and Raney Ni observed previously [32].

The XRD patterns of the Raney Ni, M-Raney Ni, RQ Ni, and MRQNi-9-10-413 catalysts are presented in Fig. 3. Both Raney Ni and M-Raney Ni only showed reflections at 2θ of 44.0°, 51.2°, and 75.5°, corresponding to the (1 1 1), (2 0 0), and (2 2 0) planes of fcc Ni [36]. For RQ Ni, besides the reflections of fcc Ni, additional reflections at 2θ of 44.2°, 65.6°, and 83.0° characteristic of the (1 1 0), (2 0 2), and (2 1 2) planes of Ni_2Al_3 were visible [36]. The existence of the residual Ni_2Al_3 phase has been reported for leaching similarly as-quenched Ni–Al [14] and Ni–P–Al alloys [13], which is ascribed to the unique microstructure of the Ni–Al alloy prepared by the rapid quenching technique [24]. The reflections of the Ni_2Al_3 phase still can be discerned in MRQNi-9-10-413, indicating that the modification did not completely eliminate the Ni_2Al_3 phase.

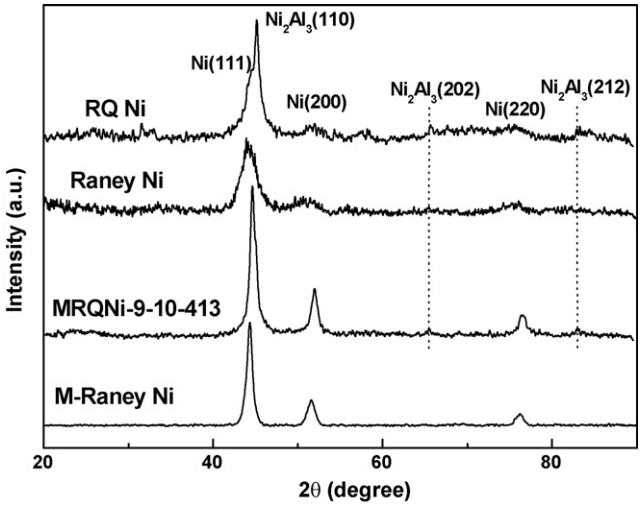

Fig. 3. XRD patterns of the RQ Ni, Raney Ni, M-Raney Ni, and MRQNi-9-10-413 catalysts.

The Ni mean crystallite sizes of the catalysts calculated by X-ray line broadening are summarized in Table 1. It is apparent that the Ni crystallite size in RQ Ni (6.8 nm) is larger than that in Raney Ni (5.6 nm). It has been proposed that because of the rapid quenching technique, more defects are generated in the RQ Ni–Al alloy, thus Ni crystallites in the resulting RQ Ni are more coordinatively unsaturated and inclined to aggregate into larger crystallites [24]. The Ni crystallite sizes in the MRQNi catalysts are larger than that in RQ Ni. It is found in Table 1 that the Ni crystallite sizes in the MRQNi catalysts were mainly dependent on the modification temperature. The higher the modification temperature, the larger the Ni crystallite size is. When the modification temperature was raised to 413 K, the Ni crystallite size in the MRQNi catalysts was increased to around 14 nm. On the contrary, the concentration of the modification solution has less distinct effect on the Ni crystallite size in the MRQNi catalysts, as evidenced by the last four entries in Table 1. It is also noted that for M-Raney Ni the Ni crystallite size was increased to ~14 nm after modification.

3.4. Surface species and chemical states

To reveal the nature of the tartrate species formed on the MRQNi catalysts, the thermal decomposition behaviors of MRQNi-9-10-413, sodium–nickel(II) tartrate, and nickel(II) tartrate were analyzed. The latter two are possible tartrate species on the MNi catalysts [8,32,37]. For comparison, the thermal decomposition behavior of M-Raney Ni catalyst is also analyzed. As shown in Fig. 4, aside from a distinct weight loss at ca. 373 K due to dehydration, decomposition of nickel(II) tartrate occurred at ca. 623 K. The total weight loss of nickel(II) tartrate was ca. 73.8%, which is in accordance with the weight loss of 76.7% reported before [32]. For sodium–nickel(II) tartrate, following the continuous weight loss from the beginning of the heating process, there was a distinct

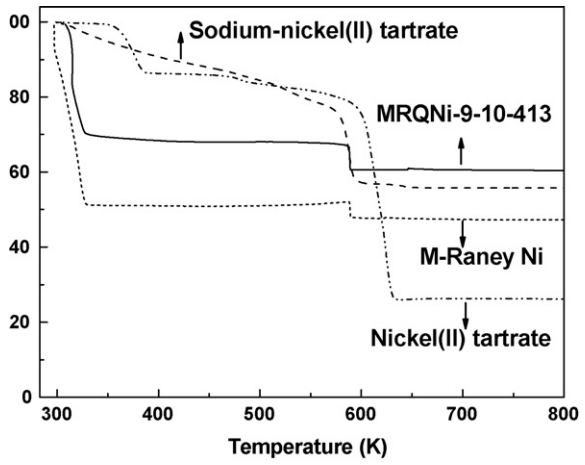

Fig. 4. TGA curves of Ni(II) tartrate, sodium–nickel(II) tartrate, M-Raney Ni and the MRQNi-9-10-413 catalyst.

weight loss at ca. 591 K, resulting in a total weight loss of 43.9% also close to the literature value [32]. For MRQNi-9-10-413 and M-Raney Ni, besides the weight loss at ca. 323 K attributable to the evaporation of methanol, another weight loss process took place at the temperature identical to that of sodium–nickel(II) tartrate, inferring the formation of this tartrate species on the MRQNi and the M-Raney Ni catalysts. As estimated by the weight loss in TGA measurements, the amounts of sodium–nickel(II) tartrate species adsorbed on the MRQNi-9-10-413 catalyst are ca. 10.5 wt.%, which is higher than that on the M-Raney Ni catalysts (8.4 wt.%). On the other hand, because the complex of sodium–nickel(II) tartrate is amorphous [32], it is not detectable in Fig. 3 by XRD.

The surface states of the RQ Ni and MRQNi catalysts were analyzed by XPS. As the Ni 2p spectra of the MRQNi catalysts are similar, the spectrum of MRQNi-9-10-413 is presented in Fig. 5a as a representative. The sodium–nickel(II) tartrate complex was used for comparison. RQ Ni only showed one sharp Ni $2p_{3/2}$ peak at 852.7 eV, indicating that nickel is predominant in the metallic state [38]. The sodium–nickel(II) tartrate complex is represented by the Ni $2p_{3/2}$ peak at 856.2 eV and a broad satellite at higher BE value, which are characteristic of the divalent paramagnetic Ni^{2+}. For the M-Raney Ni and MRQNi-9-10-413 catalysts, after curve fitting, there are three components assignable to metallic Ni with Ni $2p_{3/2}$ BE of 852.7 eV, sodium–nickel(II) tartrate with Ni $2p_{3/2}$ BE of 856.1 eV and its satellite peak with BE of 861.7 eV (Fig. 5b) [38]. Based on the curve fitting results, the surface Ni^{2+}/Ni^0 ratio on the MRQNi-9-10-413 catalyst was calculated to be 1.19, while the ratio was 0.98 on the M-Raney Ni catalyst, showing that the surface density of the sodium–nickel(II) tartrate species on the former is higher than that on the latter, which is in accordance with the TGA observations.

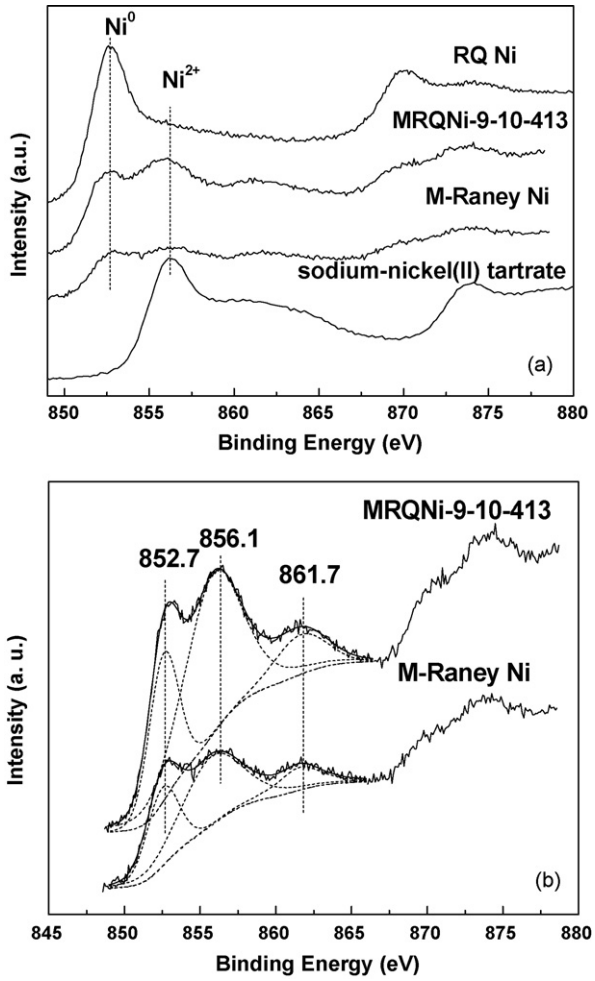

Fig. 5. (a) Ni 2p spectra of RQ Ni, sodium–nickel(II) tartrate, MRQNi-9-10-413, and M-Raney Ni, and (b) curve fitting results of the Ni 2p level of the MRQNi-9-10-413 and M-Raney Ni catalysts.

3.5. Enantioselective hydrogenation of butanone

3.5.1. Effect of the modification parameters

The catalytic results of the RQ Ni and MRQNi catalysts in liquid phase enantioselective hydrogenation of butanone are compiled in Table 2. The modification conditions are also presented in the table

Table 2
Effect of the modification conditions on the conversion and enantioselectivity over the MRQNi catalysts.[a].

Catalyst	Modification condition				Conversion (%)	ee_{max} (%)
	W_{TA} (g)	W_{NaBr} (g)	V_{H_2O} (ml)	T (K)		
RQ Ni	–	–	–	–	99.9 (1 h)	0 (1 h)
TA-MRQNi	0.4	0	40	373	17.1	5.6
M-Raney Ni	0.4	6	40	373	18.0	19.4
MRQNi-6-40-373	0.4	6	40	373	45.1	9.8
MRQNi-9-40-373	0.4	9	40	373	50.0	12.4
MRQNi-9-40-383	0.4	9	40	383	48.2	15.0
MRQNi-9-40-393	0.4	9	40	393	45.6	17.5
MRQNi-9-40-403	0.4	9	40	403	43.4	20.3
MRQNi-9-40-413	0.4	9	40	413	40.1	22.7
MRQNi-9-30-413	0.4	9	30	413	39.2	24.3
MRQNi-9-20-413	0.4	9	20	413	38.6	27.5
MRQNi-9-10-413	0.4	9	10	413	36.5	29.8

[a] Reaction conditions: T = 333 K, P_{H_2} = 9 MPa, and t = 6 h. Other reaction conditions are described in Section 2.3.

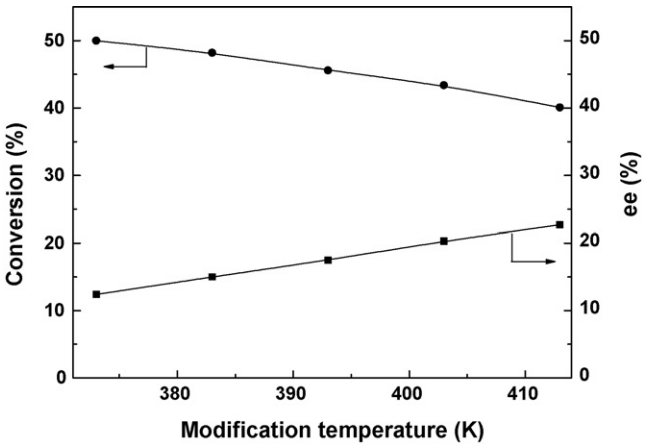

Fig. 6. Dependence of the conversion and enantioselectivity on the modification temperature over the MRQNi-9-40-*z*-series catalysts.

for clarity. Over RQ Ni, the reactant was nearly completely converted to 2-butanol within 1 h, but with no enantioselectivity being observed. When being modified with TA only, the resulting TA–RQ Ni catalyst exhibited a much lower activity, giving a conversion of only 17.1% after a reaction time as long as 6 h with an ee value of 5.6%. It has been reported that the addition of a co-modifier NaBr to the modification solution can effectively improve the enantioselectivity of the MNi catalysts in reactions such as hydrogenation of 2-octanone and methyl acetoacetate [5,39], so we modified RQ Ni with a combination of TA and NaBr.

We first attempted the typical modification condition for Raney Ni [5,28] to prepare the MRQNi catalyst; the resulting catalyst is MRQNi-6-40-373. As shown in Table 2, the butanone conversion over MRQNi-6-40-373 at a reaction time of 6 h was 45.1%, which is substantially higher than that over TA–RQNi modified by TA only. However, the ee value was still low (9.8%), although it has been improved somewhat relative to TA–RQNi. For the control M-Raney Ni catalyst, a much higher ee value of 19.4% was obtained, showing that the typical modification condition for Raney Ni is not suitable for RQ Ni.

Fig. 6 shows the effect of the modification temperature on the conversion of butanone and enantioselectivity over the MRQNi-9-40-*z*-series catalysts. When the modification temperature was raised from 373 to 413 K, the butanone conversion decreased from 50.0% to 40.1%, while the ee value increased almost linearly from 12.4% to 22.7%. The decrease in the activity with the modification temperature may be attributed to the fact that the MRQNi catalyst prepared at higher modification temperature possessed lower BET surface area accessible by the reactants (Table 1). As to the factors affecting the enantioselectivity, Harada et al. suggested that the Al species on the catalyst surface is adverse to the enantioselectivity over the chirally modified Raney Ni catalyst, and the removal of which is important for obtaining a highly enantioselective catalyst for the hydrogenation of methyl acetoacetate [14]. Tai and Harada also demonstrated that the surface Al content affected the enantioselectivity [6]. In order to enhance the enantioselectivity, they introduced ultrasound irradiation to the preparation of Raney Ni based on the idea that most Al species could be removed in this way [40]. As verified by elemental analysis, the higher the modification temperature is, the lower the Al content on the catalyst surface is (Table 1). On the other hand, Table 1 shows that higher modification temperature led to larger Ni crystallite size in the MRQNi catalyst. It has been revealed by Nitta et al. that the catalyst made of larger Ni crystallite tended to afford the higher enantioselective ability [16]. Similarly, Osawa et al. observed that larger Ni crystallite size was favorable for attaining higher optical yields [27]. Thus, the lower surface Al content and the larger Ni crystallite size may account for the higher enantioselectivity of the MRQNi catalyst modified at higher temperature.

As to the influence of the concentration of the modification solution on the catalytic performance of the MRQNi catalyst, Table 2 shows that higher concentration led to lower conversion and higher enantioselectivity. Over the MRQNi-9-40-413 catalyst, the butanone conversion was 40.1%, and the ee value was 22.7%. Over the MRQNi-9-10-413 catalyst, the butanone conversion was decreased to 36.5%, while the ee value was increased to 29.8%. It is expected that with the increment of the concentration of TA, more tartrate species were formed and adsorbed on the catalyst surface, resulting in lower activity but higher enantioselectivity [39]. Moreover, more concentrated modification solution contributed to lower surface Al content and larger Ni crystallite size, which are also beneficial to the enantioselectivity as demonstrated by the last four entries in Table 2.

The effect of the amount of NaBr in the modification solution on the catalytic performance of the MRQNi catalyst was also investigated. As shown by entry 4 in Table 2, when there were 6.0 g of NaBr in the modification solution, the butanone conversion of 45.1% and the ee value of 9.8% were obtained. When the amount of NaBr was increased to 9.0 g, the conversion and the ee value were increased to 50.0% and 12.4%, respectively (entry 5, Table 2). However, excessive amount of NaBr such as 12.0 g reduced both the conversion and enantioselectivity (not shown). Kukula and Červený suggested that NaBr changed the ion strength of the modification solution and decreased the concentration of H^+ ions, resulting in lower degree of Ni leaching to the modification solution, which thus preserves the activity of the chirally modified Ni catalyst in the hydrogenation of methyl acetoacetate [39]. As reported in the literature, the optimal amount of NaBr to maximize the enantioselectivity depends on the type of the Ni catalysts [41]. We found that M-Raney Ni exhibited the best catalytic performance when modified with 6.0 g of NaBr, which is less than that required for RQ Ni. The role of NaBr in enhancing the enantioselectivity has been widely studied on the chirally modified Raney Ni catalysts [5–7,39]. It is generally accepted that the Na^+ and/or Br^- ions can block the unmodified active sites for the racemic reaction, thus increasing the enantioselectivity [5,39]. Excessive NaBr will also block the chiral sites, which is detrimental to both the activity and the enantioselectivity of the MRQNi catalyst.

3.5.2. *Effect of the reaction variables*

Table 3 summarizes the butanone conversion and the enantioselectivity over the MRQNi-9-10-413 catalyst at different reaction temperature and H_2 pressure. The effect of the reaction temperature on the catalytic performance was investigated under the constant H_2 pressure of 9 MPa. It can be seen that the butanone conversion was improved when the reaction temperature was raised from 323 to 343 K, while the ee value first increased and then declined dramatically at 343 K. The occurrence of the maximum in the enantioselectivity with the reaction temperature was observed on the chirally modified Raney Ni and Ni/SiO_2 catalysts in the

Table 3
Effect of the reaction variables on the conversion and enantioselectivity over the MRQNi-9-10-413 catalyst at a reaction time of 6 h.[a].

T (K)	P_{H_2} (MPa)	Conversion (%)	ee_{max} (%)
333	3.0	16.2	14.5
333	6.0	26.4	17.3
333	9.0	36.5	29.8
323	9.0	24.3	27.1
343	9.0	50.7	13.4

[a] Other reaction conditions are described in Section 2.3.

hydrogenation of methyl acetoacetate [42,43]. Similarly, Osawa et al. found that the hydrogenations of 2-alkanones over the chirally modified Raney Ni catalyst gave higher optical yields at 333 K than those at 373 K [10].

With the reaction temperature being fixed at 333 K, it is found that when the H_2 pressure was increased from 3 to 9 MPa, the butanone conversion and the ee value over the MRQNi catalysts increased respectively from 16.2% to 36.5% and 14.5% to 29.8%. This result is similar to that of Kukula and Červený, where the optical yield increased steadily with the increment of the H_2 pressure from 1 to 10 MPa in the enantioselective hydrogenation of methyl acetoacetate over the chirally modified Raney Ni catalyst [43].

3.5.3. Comparison of the catalytic behaviors of M-Raney Ni and MRQNi

In order to have a better insight into the difference in the catalytic performances of the chirally modified Raney Ni and RQ Ni catalysts, the reaction courses of two typical catalysts, M-Raney Ni and MRQNi-9-10-413, were compared under the optimized reaction conditions of these catalysts. Fig. 7a shows that over the MRQNi-9-10-413 catalyst, the butanone conversion increased much faster than that over M-Raney Ni: after a reaction time of 6 h, the butanone conversion over the former was 36.5%, which is twice as that over the latter. Fouilloux has observed that the residual Ni_2Al_3 phase in Raney Ni is responsible for the enhancement of the hydrogenation activity [44], which may be the reason for the higher activity of the MRQNi-9-10-413 catalyst.

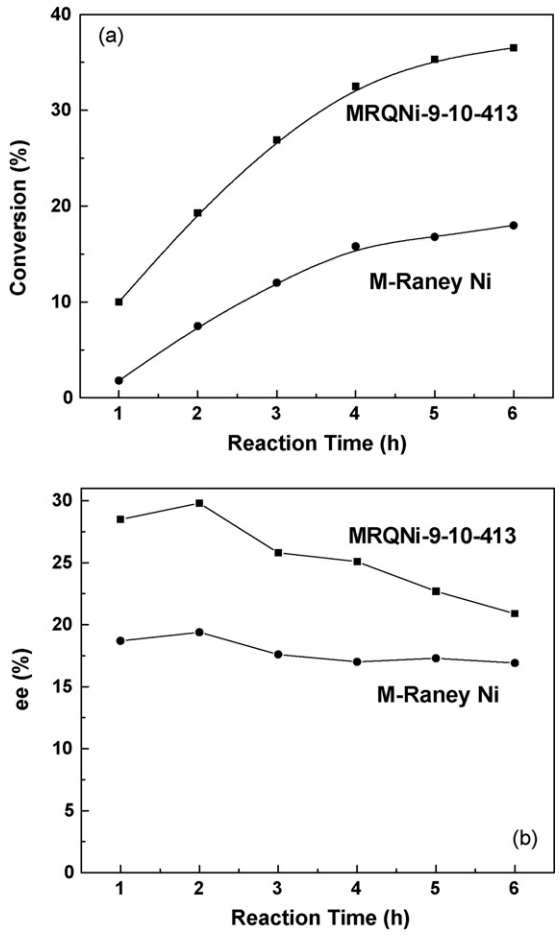

Fig. 7. The evolutions of (a) the conversion of butanone, and (b) the enantioselectivity over the M-Raney Ni and MRQNi-9-10-413 catalysts. The reaction conditions are the same as those described in Table 2.

The evolution of the enantioselectivity with the reaction time was monitored and illustrated in Fig. 7b. Over both catalysts, the ee value first increased with the reaction time, reached a maximum at the reaction time of 2 h, and then declined at prolonged time. Moreover, the ee value over the MRQNi-9-10-413 catalyst during the whole hydrogenation process was substantially higher than that over M-Raney Ni. The maximum ee value of 29.8% was obtained over the MRQNi-9-10-413 catalyst, while it was only 19.4% over M-Raney Ni.

As shown in Table 1, the MRQNi-9-10-413 catalyst has a slightly lower surface Al content and a slightly larger mean Ni crystallite size than M-Raney Ni. It has been proposed that lower surface Al content [6,14,40] and larger Ni crystallite size [16,27] are both favorable for attaining higher enantioselectivity. However, the relatively small differences in the surface Al content and the Ni crystallite size, although reproducible, may not suffice to justify the much larger difference between the ee values of the two catalysts. On the other hand, it has been proposed that the complex formed by TA is important to achieve the high enantioselectivity [8,32,37]. As revealed by the XPS measurements, the percentage of the sodium–nickel(II) tartrate complex with respect to the total amount of the surface Ni species on the MRQNi-9-10-413 catalyst is ca. 10% higher than that on M-Raney Ni, which may be one important reason underlying the higher enantioselectivity over the MRQNi catalysts.

4. Conclusions

The MRQNi catalyst derived from the rapidly quenched Ni–Al alloy can be both more active and more enantioselective than the M-Raney Ni catalyst in the liquid phase hydrogenation of butanone to R-(−)-2-butanol. As compared to M-Raney Ni, higher modification temperature and higher concentration of NaBr were needed for MRQNi to achieve the optimal enantioselectivity. The superior catalytic performance of the MRQNi catalyst to M-Raney Ni is mainly attributed to the higher surface population of the sodium–nickel(II) tartrate complex on the former, although the lower surface Al content and the larger Ni crystallite size may also have some contribution. This work, although preliminary, clearly demonstrates the prospective of the rapidly quenched Ni–Al alloy as a new category of Ni precursor for the preparation of efficient MNi catalyst for enantioselective hydrogenation of pre-chiral ketones or other carbonyl group-containing pre-chiral molecules to chiral alcohols.

Acknowledgments

This work was supported by the National Basic Research Program of China (2006CB202502), the NSF of China (20203004, 20721063, 20803009, and 20873027), the Program of New Century Excellent Talents in Universities (NCET-08-0126), and the Science & Technology Commission of Shanghai Municipality (08DZ2270500 and 09DZ2271500).

References

[1] A. Baiker, H.U. Blaser, in: G. Ertl, H. Knözinger, J. Weitkamp (Eds.), Handbook of Heterogeneous Catalysis, Wiley-VCH, Weinheim, 1997, p. 2422.
[2] G. Jannes, V. Dubois, Chiral Reactions in Heterogeneous Catalysis, Plenum Press, New York, 1995, pp. 1–2.
[3] F. Zaera, J. Phys. Chem. C 112 (2008) 16196–16203.
[4] G. Webb, P.B. Wells, Catal. Today 12 (1992) 319–337.
[5] Y. Izumi, Adv. Catal. 32 (1983) 215–271.
[6] A. Tai, T. Harada, in: Y. Iwasawa (Ed.), Tailored Metal Catalysts, Reidel, Dordrecht, 1986, p. 265.
[7] T. Osawa, T. Harada, A. Tai, Catal. Today 37 (1997) 465–480.
[8] T. Osawa, T. Harada, O. Takayasu, Top. Catal. 13 (2000) 155–168.
[9] T. Sugimura, Catal. Surv. Jpn. 3 (1999) 37–42.
[10] T. Osawa, T. Harada, A. Tai, J. Catal. 121 (1990) 7–17.

[11] J. Freel, W.J.M. Pieters, R.B. Anderson, J. Catal. 14 (1969) 247–256.
[12] T. Harada, Y. Izumi, Chem. Lett. (1978) 1195–1196.
[13] L.H. Gross, R. Rys, J. Org. Chem. 39 (1974) 2429–2430.
[14] T. Harada, S. Onaka, A. Tai, Y. Izumi, Chem. Lett. (1977) 1131–1132.
[15] T. Harada, Y. Imachi, A. Tai, Y. Izumi, Metal–Support and Metal–Additive Effects in Catalysis, Elsevier Science, New York, 1982, p. 377.
[16] Y. Nitta, F. Sekine, T. Imanaka, S. Teranishi, Bull. Chem. Soc. Jpn. 54 (1981) 980–984.
[17] H. Brunner, M. Muschiol, T. Wischert, Tetrahedron: Asymmetry 1 (1990) 159–162.
[18] Y. Izumi, M. Imaida, T. Harada, T. Tanabe, S. Yajima, T. Ninomiya, Bull. Chem. Soc. Jpn. 42 (1969) 241–243.
[19] K. Klement, R.H. Willens, P. Duwez, Nature 187 (1960) 869–870.
[20] Á. Molnár, G.V. Smith, M. Bartók, Adv. Catal. 36 (1989) 329–383.
[21] G.A. Somorjai, Catal. Rev. Sci. Eng. 18 (1978) 173–181.
[22] B. Liu, M.H. Qiao, J.F. Deng, K.N. Fan, X.X. Zhang, B.N. Zong, J. Catal. 204 (2001) 512–515.
[23] H.R. Hu, M.H. Qiao, Y. Pei, K.N. Fan, H.X. Li, B.N. Zong, X.X. Zhang, Appl. Catal. A: Gen. 252 (2003) 173–183.
[24] H.R. Hu, M.H. Qiao, S. Wang, K.N. Fan, H.X. Li, B.N. Zong, X.X. Zhang, J. Catal. 221 (2004) 612–618.
[25] H.R. Hu, F.Z. Xie, Y. Pei, M.H. Qiao, S.R. Yan, H.Y. He, K.N. Fan, H.X. Li, B.N. Zong, X.X. Zhang, J. Catal. 237 (2006) 143–151.
[26] F.Z. Xie, X.W. Chu, H.R. Hu, M.H. Qiao, S.R. Yan, Y.L. Zhu, H.Y. He, K.N. Fan, H.X. Li, B.N. Zong, X.X. Zhang, J. Catal. 241 (2006) 211–220.
[27] T. Osawa, S. Mita, A. Iwai, O. Takayasu, H. Hashiba, S. Hashimoto, T. Harada, I. Matsuura, J. Mol. Catal. A 157 (2000) 207–216.
[28] T. Harada, M. Yamamoto, S. Onaka, M. Imaida, H. Ozaki, A. Tai, Y. Izumi, Bull. Chem. Soc. Jpn. 54 (1981) 2323–2329.
[29] E.P. Barrett, L.G. Joyner, P.P. Halenda, J. Am. Chem. Soc. 73 (1951) 373–380.
[30] B.E. Warren, J. Appl. Phys. 12 (1941) 375–383.
[31] S.D. Robertson, R.B. Anderson, J. Catal. 23 (1971) 286–294.
[32] P. Kukula, L. Červený, Appl. Catal. A: Gen. 223 (2002) 43–55.
[33] M.L. Bakker, D.J. Young, M.S. Wainwright, J. Mater. Sci. 23 (1988) 3921–3926.
[34] J. Masson, P. Cividino, J. Court, J. Mol. Catal. A 111 (1996) 289–295.
[35] J.H. de Boer, in: D.H. Everett, F.S. Stone (Eds.), The Structure and Properties of Porous Materials, Butterworth, London, 1958, p. 68.
[36] PDFMaint Version 3.0, Powder Diffraction Database, Bruker Analytical X-ray Systems GmbH, 1997.
[37] A. Hoek, W.M.H. Sachtler, J. Catal. 58 (1979) 276–286.
[38] J.F. Moulder, W.F. Stickle, P.E. Sobol, K.D. Bomben, in: J. Chastain (Ed.), Handbook of X-ray Photoelectron Spectroscopy, Perkin-Elmer, Eden Prairie, MN, 1992.
[39] P. Kukula, L. Červený, Appl. Catal. A: Gen 210 (2001) 237–246.
[40] A. Tai, T. Kikukawa, T. Sugimura, Y. Inoue, S. Abe, T. Osawa, T. Harada, Bull. Chem. Soc. Jpn. 67 (1994) 2473–2477.
[41] T. Harada, A. Tai, M. Yamamoto, H. Ozaki, Y. Izumi, Stud. Surf. Sci. Catal. 7 (1981) 364–375.
[42] M.A. Keane, Langmuir 13 (1997) 41–50.
[43] P. Kukula, L. Červený, J. Mol. Catal. A 185 (2002) 195–202.
[44] P. Fouilloux, Appl. Catal. 8 (1983) 1–42.